Technical Application of Fracture Mechanics to Thin-Walled Structures

By Hiroshi Kihara
Professor, Director, Welding Research Institute, Osaka University, Yamada-ue, Suita, 565, Japan
and Kazuo Ikeda
Deputy Manager, Structural Engineering Laboratory, Kobe Steel, Ltd., Doi, Amagasaki 660, Japan

1. Introduction

Ships, bridges, storage tanks, pressure vessels, pipelines, and rocket motor casings are examples of the type of large thin-walled structures in which brittle failures have been reported.

In general, the notch is needed for brittle fracture initiation, and the welded joint in welded structures, where the weld cracks or various kinds of weld defects are frequently located, becomes an origin of brittle fracture initiation. The welded joint is embritted by welding thermal cycles and high welding residual stress is superposed at the cross joint. In addition, such mis-fabrication as the excess welding heat input, the angular distortion and the misalignment result in remarkably great increase in brittle fracture initiation temperature. Consequently, catastrophic brittle failure may initiate at service temperature experienced.

It may be needed for the safety design of structures from viewpoint of brittle fracture that effect of various factors on the brittle fracture initiation characteristics is revealed, and what kinds of factor are to be taken into account, then the brittle fracture initiation temperature can be estimated theoretically. Meanwhile, arrangement of crack arrester in ships, design of pipelines and reactor pressure vessels should be based on the brittle fracture propagation and arresting characteristics.

2. Crack size

2.1 Through-thickness notch (Notch length)

The Griffith-Orowan energy equation for the initiation of unstable notch of length 2c being subjected to a uniform tensile stress below yield stress, σ, at infinity is expressed by the following equation:

$$\frac{\pi\sigma^2 c}{E} = 2S_i \qquad (1)$$

where E = Young's modulus, S_i = plastic surface energy.

Since it is impossible to employ a infinitely wide specimen in laboratory, the deep notch test specimen as shown in Fig.1 is employed. According to Ikeda et al.,[1] in the temperature region of low-stress brittle fracture, the following modified Griffith-Orowan energy equation for finite width can be applied:

$$\frac{\pi\{f(\gamma)\sigma\}^2 c}{E} = 2S_i \qquad (2)$$

where $f(\gamma) = \sqrt{\frac{2}{\pi\gamma}\left(\tan\frac{\pi\gamma}{2} + 0.1\sin\pi\gamma\right)} \qquad \gamma = c/b \qquad (3)$

c = notch length, b = half width of specimen.

The evaluations of steel quality against brittle fracture initiation for the base metal, the bond (or the fusion line), and the weld metal are conducted by using the deep notch test specimen as shown in Figs.1(a) and (b),[2] respectively.

Substituting the gross fracture stress at various temperatures in the temperature zone, where the net fracture stress on the notch section is lower than the yield stress at temperature concerned, into Eq.(2), the plastic surface energy for fracture initiation, S_i, can be obtained. A linear relationship between the logarithm of S_i and a reciprocal of absolute temperature exists as expressed by the following equation:

$$S_i = S_{oi} e^{-2k_i/T_k} \qquad (4)$$

where T_k = absolute temperature, S_{oi}, k_i = material constant.

When the design stress, σ, is 1/n of yield stress for base metal at room temperature, the stress is expressed by

$$\sigma = \{\sigma_y\}_{B.M.-R.T.}/n \qquad (5)$$

When the design stress is 1/n of yield stress for the steel quality concerned at fracture temperature, the stress is expressed by

$$\left.\begin{aligned} \sigma &= \sigma_y/n \\ \sigma_y &= \sigma_{oy} e^{k_y/T_k} \end{aligned}\right\} \qquad (6)$$

where σ_{oy}, k_y = material constant.

From Eq.(1) through Eq.(6), the brittle fracture initiation temperature for a crack of 2c long in an infinite plate can be obtained by the following equation:

$$e^{2(k_i+k_y)/T_k} = \frac{2E}{\pi}\cdot\frac{S_{oi}}{\sigma_{oy}^2}\cdot\frac{n^2}{c} \qquad (7)$$

The brittle fracture initiation characteristics of base metal in an infinite plate for mild steel, various kinds of high strength steels (HT60, HT70, HT80, HT100) and low temperature steels (Aluminum killed steel quenched and tempered, 2.5% Ni, 3.5% Ni, 9% Ni steels) are shown in Fig.3.[1] It is noted in the figure that the brittle fracture initiation temperature increases with crack length, the low temperature steels (Steels L,M,N,P) show very good quality, and HT100 (Steel H) shows higher initiation temperature than the other kinds of steel.

Fracture toughness of ultra-high strength steel for rocket motor casing etc. can be evaluated by using the symmetrical center cracked plate as shown in Fig.4 and the following equation can be applied:[3]

$$K_c = \sigma\sqrt{\pi a_0}\sqrt{\frac{2}{\pi\gamma}\tan\frac{\pi\gamma}{2}} \qquad \gamma = 2a_0/W \tag{8}$$

where a_0 = half notch length, W = width of specimen.

In general, the welded joint is more brittle than the base metal and influenced by the welding procedures and the heat input. In addition, possibility of existence of crack along the bond or in the weld metal is high. Therefore, the brittle fracture initiation characteristics of bond and weld metal are very significant. The brittle fracture initiation characteristics of base metal, bond and weld metal for HT80 and HT60, which were evaluated by using the deep notch test with welded joint as shown in Fig.1(b), are shown in Figs.5 and 6, respectively.[2] It is noted in Fig.5 that the embrittlement of bond for some HT80 by automatic sumberged-arc welding is serious with increased welding heat input. An increase in brittle fracture initiation temperature $[T_i]_{c=40,\ \sigma_y/2.5}$ of bond from that of base metal with heat input for HT60 (Steels A~G), HT70 (Steel H) HT80 (Steels I~L) and HT100 (Steel M) is shown in Fig.7.[2] It is noted that the welding heat input control is needed not for HT60 but needed for some HT70 and HT80.

2.2 Surface notch (Notch depth)

The wide plate test specimen with a surface notch of various depths produced by machining was pulled to fracture at various temperatures. The correlation between the fracture stress and the ratio of notch depth to plate thickness, t_1/t, at the same temperature is shown in Fig.8 and expressed by the following equation:[4]

$$\sigma\cdot(t_1/t) = \text{const} = \sigma_o \tag{9}$$

where σ_o = fracture stress for through-thickness.

According to Irwin,[5] the fracture toughness for surface notch, K_{IC}, is expressed by

$$K_{IC}^2 = \frac{1.2\sigma^2}{\Phi^2 - 0.212(\sigma/\sigma_y)^2}\cdot 2t\cdot\tan\frac{\pi t_1}{2t} \tag{10}$$

where

$$\Phi = \int_0^{\pi/2}\sqrt{1-\left(\frac{c^2-t_1^2}{c^2}\right)\sin^2\theta}\cdot d\theta \qquad \text{for } \frac{t_1}{t} < 0.5 \tag{11}$$

It has been found from the test results for various welding procedures that the sharp corner at the toe of reinforcement in laterally welded joint without any surface notch has a equivalent notch depth, t', of 0.3~1.5mm.[6]

3. Angular distortion

When two plates are welded not in a plane but with angular distortion due to mis-fabrication, the brittle fracture initiation temperature increases with angular distortion for HT80 welded by submerged arc welding with heat input of 40,000 Joule/cm as shown in Fig.9.[7]

4. Superposition of angular distortion or misalignment on surface notch

In case of the superposition of angular distortion or misalignment, stress intensity factor, K_{IC} is expressed by the following equations:[6][8]

For notch length less than 15 times plate thickness

$$K = K_p + K_B$$

$$= f(c/b)\frac{t_1}{t}\sigma\sqrt{\pi c}+6\frac{f(c/b)}{f(t_1/t)}Y_B\frac{e\varkappa_e+d\varkappa_d}{t}\frac{t_1}{t}\sigma\sqrt{c} \tag{12}$$

For very long crack

$$K = f(t_1/t)\sigma\sqrt{\pi t_1}+6Y_B\frac{e\varkappa_e+d\varkappa_d}{t}\sigma\sqrt{t_1} \tag{13}$$

For toe of reinforcement in laterally welded joint without surface notch, the equivalent notch depth, t_1' should be taken instead of t_1 in Eq.(13).

where $m = \sqrt{3(1-\nu^2)\frac{\sigma}{E}\cdot\frac{\ell}{t}}$ (14)

c = half length of surface notch, b = half width of specimen,

t_1/t = ratio of notch depth to plate thickness, e = angular distortion for span ℓ, d = misalignment, ν = Poisson's ratio, $f(\gamma)$, Y_B, κ_d, κ_e, are shown in Fig.10(a)~(d).

The brittle fracture initiation temperature increases by several times 10°C, with angular distortion depending on the ratio of notch depth to plate thickness.

5. Welding residual stress

When the maximum tensile residual stresses in the direction of longitudinal joint for longitudianl joint and cross joint are denoted by σ_1 and σ_2, respectively, the ratios of σ_1 and σ_2 to guaranteed yield stress, σ_y, for various high strength steels are presented in Table 1.[2)]

When the welding residual stress is superposed on the notch, its stress intensity factor is greater than that without residual stress as shown in Fig.11, and the brittle fracture initiation temperature increases by several times 10°C by superposition of residual stress. The effect of residual stress on an increase in brittle fracture initiation temperature is found in the zone of shadow lines for c = 20 or 40 mm for the yield stresses 50, 60, 70, 90 kg/mm^2 which represent 60-, 70-, 80-, 100 kg/mm^2 high strength steels, respectively.

6. Stress-relieving heat treatment

Although the stress-relieving heat treatment results in an increase in fracture stress due to the relieving of residual stress, the steel quality is influenced by the heat treatment. Change in brittle fracture initiation temperature of bond $[T_i]_{c=40}$ caused by stress relieving treatment with various heat inputs for $\sigma = \sigma_y$(bond)/2.5 is shown by arrows in Fig.13. The upward and the downward arrows indicate respectively the increase and decrease in brittle fracture

initiation and their magnitudes. An example of base metal is shown only at the furthest left side. For all cases, except the case of HT70 at 40,000 Houle/cm, cooling was carried out in a furnace. Embrittlement caused by stress-relieving heat treatment is at a maximum of 20°C. In addition, it is found that air cooling is better than furnace cooling. However, it has been found for HT80 experimentally that the weld metal deposited by sumberged arc welding is sometimes embrittled seriously by stress-relieving treatment.

7. Prestraining

In general, the prestrain in bending of plates in fabrication of welded structures is at a maximum of 2 to 3%. It is proved that the effect of difference in loading such as bending and tension on the embrittlement of steel is negligibly small. Therefore, the deep notch test specimens taken from prestrained plate have been tested. The correlation between the prestrain and the increase in brittle fracture initiation temperature of prestrained plate from the virgin material for c = 40 mm, $\sigma = \sigma_y$(base metal)/2.5 for mild steel, 60, 80 and 100 kg/mm^2 high strength steels and 9% Ni steel is shown in Fig.14.[9)] It is noted that the embrittlement caused by prestrain for HT60 and HT80 is relatively small. However, it has been found experimentally that the prestrained weld metal deposited by submerged **arc welding for HT80** results sometimes in serious embrittlement.

8. Curvature

If the effect of curvature of curved plate in cylindrical vessels, pipes and spherical vessels on the brittle fracture initiation characteristics is found, the fracture stress for curved plate with any curvature can be estimated from that for flat plate in deep notch test. The line pipe with a through-thickness axial notch is pressurized to fracture at various low temperatures. The ratio of fracture stress of cylindrical vessel to that of flat plate, σ_p/σ_f, is given theoretically by Folias[10])

$$\frac{\sigma_p}{\sigma_f} = \frac{1}{\sqrt{1 + 1.61(c^2/Rt)}} \qquad (15)$$

where 2c = crack length, R = radius of cylindrical vessel, t = wall thickness.

The following equation is frequently applied:[11])

$$K_{cr}^{\ 2} = \frac{\pi\sigma^2 c}{\cos\theta}\left(1+\frac{5\pi\lambda^2}{32}\right)\left(\frac{4-K}{2}\right) \qquad (16)$$

where K_{cr} = critical stress intensity factor, $\lambda^2 = \frac{c^2}{Rt}\sqrt{12(1-\nu^2)}$, $\theta = \frac{\pi\sigma}{2\sigma_c}$, σ = hoop stress, $\sigma_c = \frac{1}{2}$[(Yield stress)+(tensile strength)], $K = 3-4\nu$ for plane strain, $K = \frac{3-\nu}{1+\nu}$ for plane stress, ν = Poisson's ratio.

The correlation between the fracture stress ratio of σ_p/σ_f and the parameter of 2c/R, which was experimentally determined by using many line pipes with various wall thickness, diameter and notch length, for the same temperature, plate thickness and notch length, is shown in Fig.15 and expressed by the following empirical formula:

$$\frac{\sigma_p}{\sigma_f} = \frac{1}{\sqrt{1 + 2.3(2c/R)^2}} \qquad (17)$$

Parameter 2c/R might be more preferable than c^2/Rt because the effect of plate thickness on brittle fracture initiation characteristics was not found in the test.

When a surface notch with depth of t_1 exists in line pipe, the correlation between the fracture stress at a temperature and the ratio of notch depth to wall thickness, t_1/t, is expressed experimentally by the following equation as well as Eq.(9) in the case of flat plate:[12])

$$\sigma \cdot (t_1/t) = \text{const} = \sigma_o \qquad (18)$$

where σ_o = hoop stress at fracture for through-thickness notch.

It is well-known that the difference in pressuring medium such as the liquid and the gas results in the same fracture stress and different brittle fracture propagating characteristics.

9. Structural discontinuity

When a notch is located in the region of stress concentration, where the plastic strain exists locally due to stress discontinuity, the linear fracture mechanics cannot be applied, but the COD concept should be introduced. COD criteria in the region of plastic strain is proposed by Burdekin et al.[13]) Recently, a series of experimental checking of Burdekins' proposal, and study on the brittle fracture initiation characteristics of a three dimensional model with a notch, which modifies a part of ship structure, are planned at a committee, Shipbuilding Research Association of Japan. The results will be expected for their application to ship structures, nozzle of pressure vessels, bridges and other structures.

10. Estimation of $[T_i]$ and K_{IC} from results of small size test

Although the brittle fracture initiation temperature, $[T_i]_{c=40}$, and the critical stress intensity factor, K_{IC}, obtained by using deep notch test specimen can be estimated from the stress intensity factor, K, and the stress or COD value by using various notched test specimen, the estimation from V Charpy test data is more desirable practically. Since the wide plate test specimen such as deep notch test specimen is generally in full thickness, the effect of plate thickness should be taken into account for good relationship with V Charpy test data.

For base metal, bond and weld metal, respectively, a correlation between 50% FATT in V Charpy test, $_{V}T_{rs}$, and $[T_i]_{c=40}$, $\sigma_Y/2$ in deep notch test is expressed numerically by the following equation:[14])

$$[T_i]_{c=40,\sigma_y/2} = 0.687\frac{\sigma_y}{\sigma_u}\ {}_vT_{rs}+7.83\sqrt{t}-54(^{\circ}K) \quad (19)$$

where σ_y/σ_u = yield ratio, t = plate thickness.

For bond only, a correlation between K_{IC} for 40 mm thick, which is obtained by applying Eq.(25), and V Charpy energy, ${}_vE$(kgm), at the same temperature in the transition region can be expressed by the following equation:[6]

$$\left(\frac{K_{IC}}{100}\right)^2 = 300\left(\frac{{}_v\bar{E}}{\sigma_y}\right) \quad (20)$$

From $[T_i]$ by Eq.(19) or K_{IC} by Eq.(20) and the effect of various factors on the brittle fracture initiation characteristics, proper ${}_vT_{rs}$ or ${}_vE$ in V Charpy test needed for safety design of welded structures can be determined under given boundary conditions.

11. Arrest of propagating brittle crack

The brittle crack propagates at high speed. It is well known that the crack speed increases with decreased temperature, increased stress and decreased steel quality. It is needed for arresting a propagating brittle crack at high speed to reduce the crack speed down to the critical crack speed for propagation of 150-300m/sec.[15] As the laboratory test, in general, Robertson test, double tension test and ESSO test with temperature gradient are conducted. A linear relationship between the logarithm of critical stress intensity factor for crack arrest, K_c, obtained from Eq.(21), and a reciprocal of arresting temperature in absolute temperature, T_k, is expressed by Eq.(23)[16]

$$K_c = f(\gamma)\,\sigma\sqrt{\pi c} \quad (21)$$

$$f(\gamma) = \sqrt{\frac{2}{\pi\gamma}\tan\frac{\pi\gamma}{2}}, \quad \gamma = c/b \quad (22)$$

$$K_c = K_o e^{-k/T_k} \quad (23)$$

where c = arrested crack length, b = specimen width, K_o, k = material constant.

12. Crack arrester

In the design of ship structure, the better quality steel is arranged at the gunwale and the bilge as the crack arrester so as to arrest a propagating crack at high speed. In Fig.16, a brittle crack initiated by means of wedge impact at V notch of wide crack arrester specimen under uniform temperature and applied stress propagates downward and the long brittle crack is or not arrested in the arrester plate of Grade E steel (or normalized killed steel) depending on the crack length, the temperature and the applied stress.[17]

The correlation between the applied stress and the critical temperature for crack propagation-arrest plate for various crack lengths of 500, 750 and 1,000 mm, respectively, which is the distance between the edge of brittle crack initiation side and the welded joint with crack arrester plate, is shown in Fig.17. It will be noted in the figure that the crack arresting characteristics of Grade E steel as the crack arrester for propagating long crack at the lowest service temperature of $0^{\circ}C$ and the level of half yield stress should be discussed. The correlation between the length of propagating brittle crack down to the arrester plate, c, and the effective crack length for arrest, c_{effect}, which is determined from the requested critical stress intensity factor for arrest expressed by $K_c = \sigma\sqrt{c_{effect}}$, is shown in Fig.18 and expressed by

$$c_{effect} = 0.1c + 190 \text{ (mm)} \quad (24)$$

When the steel quality and the design stress are given, the proper arrangement or the distance between Grade E steels as the crack arrester, c, can be determined. When c is given, the requested K_c at the lowest service temperature of 0°C can be determined from Eq.(24).

13. Effect of plate thickness

In general, the notch ductility decreases with increased plate thickness. The brittle fracture initiation characteristics from a crack under static tension is evaluated by the deep notch test and the arresting characteristics is evaluated by such crack arrest test as double tension test or ESSO test with temperature gradient. Correlations between the brittle fracture initiation temperature, $[T_i]_{c=40,\ \sigma_y/2.5}$, arresting temperature, $[T_a]_{c=10,100,\ \sigma_y/2}$, and the plate thickness, and the change in these temperatures per 1 mm thick are shown in Figs.19 and 20.[18][19][20] It is noted that the change rate is serious for less than 3.2 mm thick and small for greater than 35 mm thick.

In the WES specification for low temperature structural steel, WES-136,[16] the brittle fracture arresting characteristics for any thick plate (10~50 mm) is evaluated from the effect of plate thickness which is based on that for 30 mm thick plate. Effect of plate thickness is found not in material constant, k, but in K_o in Eq.(23).

The plate thickness coefficient $f_a(t)$ for arrest is defined as the ratio of K_o for any thickness to K_o for 30 mm thick, $K_o(30)$, as the basic value, and is expressed by the following equation for plate thickness of 10~50 mm:

$$K_c(t,\ T_k) = f_a(t)K_o(30)e^{-k/T_k} \qquad (24)$$

The plate thickness coefficient for brittle fracture initiation and arrest, $f_i(t)$ and $f_a(t)$, respectively, for plate thickness greater than 10 mm is proposed as follows:

$$f_i(t) = 1-0.043(t-40) \quad {}^{6)} \qquad t = 10\sim40 \text{ mm} \qquad (25)$$

$$= 1-\frac{1}{320}(t-30) \quad {}^{19)} \qquad t = 35\sim200 \text{ mm} \qquad (26)$$

$$f_a(t) = 1-\frac{1}{20}(t-30) \quad {}^{16)} \qquad t = 10\sim35 \text{ mm}$$

$$= 0.75 \quad {}^{6)} \qquad t \geqq 35 \text{ mm} \qquad (27)$$

$$= 1-\frac{1}{230}(t-30) \quad {}^{19)} \qquad t = 35\sim200 \text{ mm} \qquad (28)$$

14. Estimation of K_c and T_a from results of small size test

The critical stress intensity factor for arrest, K_c, and the arresting temperature, T_a, evaluated by using the wide plate test specimen with temperature gradient, can be estimated from such criteria as 50% FATT in pressed notch Charpy test, $_pT_c$, 50% FATT in V Charpy test, $_vT_{rs}$, NDT temperature in NRL drop weight test for nuclear pressure vessels.

In WES-136,[16] a list of requested energy transition temperature in V Charpy test, $_vT_{rE}$, is presented for any given stress level and service temperature by combining the relationships between K_c, $_pT_c$ in pressed notch Charpy test, $_vT_{rs}$ and $_vT_{rE}$ in V Charpy test, respectively.

50% FATT in drop weight tear test (DWTT) applied for evaluation of fracture toughness of line pipes is closely related with $_pT_c$ and $_vT_{rs}$, therefore, with the brittle fracture speed and the brittle fracture arresting characteristics.[11]

References

(1) K. Ikeda, Y. Akita and H. Kihara, the Deep Notch Test and Brittle Fracture Initiation, Weld. J. 46, 3 (1967) 133s: I.I.W.Doc. No. X-404-67 (1967)

(2) K. Ikeda and H. Kihara, Brittle Fracture Strength of Welded Joint, Weld. J., 49 3 (1970) 106s: I.I.W.Doc. No.X-521-69 and 1X-649-69 (1969)

(3) J. Srawley and W. Brown Jr., Fracture Toughness Testing, NASA Tech. Memo TMX-52030 (1964)

(4) K. Ikeda, H. Maenaka, Effect of Notch Size on Brittle Fracture Initiation Characteristics, Preprint of paper, Spring Meeting, Ship Research Institute, (1968) 186

(5) G.R. Irwin, Crack Extension Force for a Part-Through Crack in a Plate, J. Appl. Mech., 84E (1962) 651

(6) T. Ito, K. Tanaka and M. Sato, Effect of Plate Thickness on Brittle Fracture Initiation from Surface Notch in Weld Fusion Line, J. Soc. Nav. Arch. Japan, 131 (1972) 335

(7) Y. Akita, T. Maeda and T. Yada, On Brittle Fracture Initiation Characteristics to Welded Structures (2nd Report), J. Soc. Nav. Arch. Japan, 118 (1965) 171

(8) T. Yada, On Brittle Fracture Initiation Characteristic to Welded Structures, J. Soc. Nav. Arch. Japan, 119 (1966) 134

(9) K. Ikeda, H. Maenaka and M. Sakuma, Effect of Prestrain on Brittle Fracture Initiation Characteristics, J. Japan Weld. Soc., 38 8 (1969) 840

(10) E.S. Folias, An Axial Crack in a Pressurized Cylindrical Shell, Int. J. Fracture Mech., 1 (1963)

(11) A. Duffy, R. Eiber, W. Maxey and G. McClure, Research on Steels for High Pressure Pipelines, Fifth Int. Pipes and Pipeline Engineering Convention, London (1968)

(12) H. Kihara, K. Ikeda, N. Hisamitsu and H. Iwanaga, Brittle Fracture Initiation Characteristics of Line Pipe, Presented to American Weld. Soc. (1970)

(13) F. Burdekin and M. Dawes, Practical Use of Linear Elastic and Yielding Fracture Mechanics with Particular Reference to Pressure

Vessels, Practical Application of Fracture Mechanics to Pressure Vessel Technology, London (1971) 28

(14) Y. Kasamatsu, M. Kohno and M. Matsuoka, Relation between Charpy Test and Deep Notch Test, To be presented at 1972 Fall Meeting of Japan Weld. Soc., (1972)

(15) Y. Akita and K. Ikeda, On Brittle Crack Propagation and Arrest-Theoretical and Experimental Analyses of ESSO Test with Temperature Gradient, I.I.W.Doc. IX-364-63 (1963)

(16) WES-Specification-136, Qualification of Steel Quality for Low Temperature Steel, Japan Weld. Eng. Soc., (1964)

(17) H. Kihara, T. Kanazawa, K. Ikeda, T. Okabe and H. Yajima, Study on Welded-Type Crack Arrester (First Report), I.I.W.Doc.X-618-71 (1971)

(18) Research Committee for Iron and Steel, Studies on Criterion for Steel Quality of Preventing Welded Structures from Brittle Fracture, Japan Weld. Eng. Soc. (1962)

(19) K. Ikeda and K. Komoda, Brittle Fracture Initiation and Arresting Characteristics for Very Thin Plate, Kobe Steel Engineering Reports, 21 4 (1971) 20

(20) K. Ikeda and K. Komoda, Effect of Plate Thickness on Brittle Fracture Initiation and Arresting Characteristics for Very Thick Plate, Kobe Steel Engineering Reports, 22 2 (1972) 101: To be presented at 3rd Int. Conf. on Fracture, München (1973)

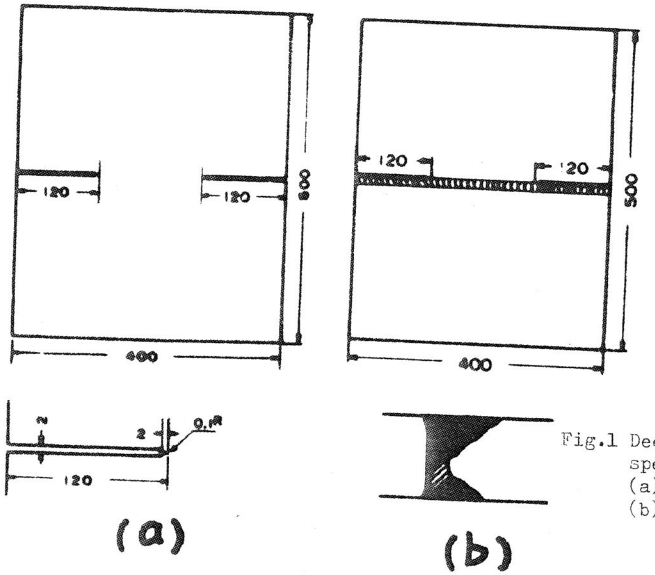

Fig.1 Deep notch test specimen
(a) base metal
(b) bond (weld metal)

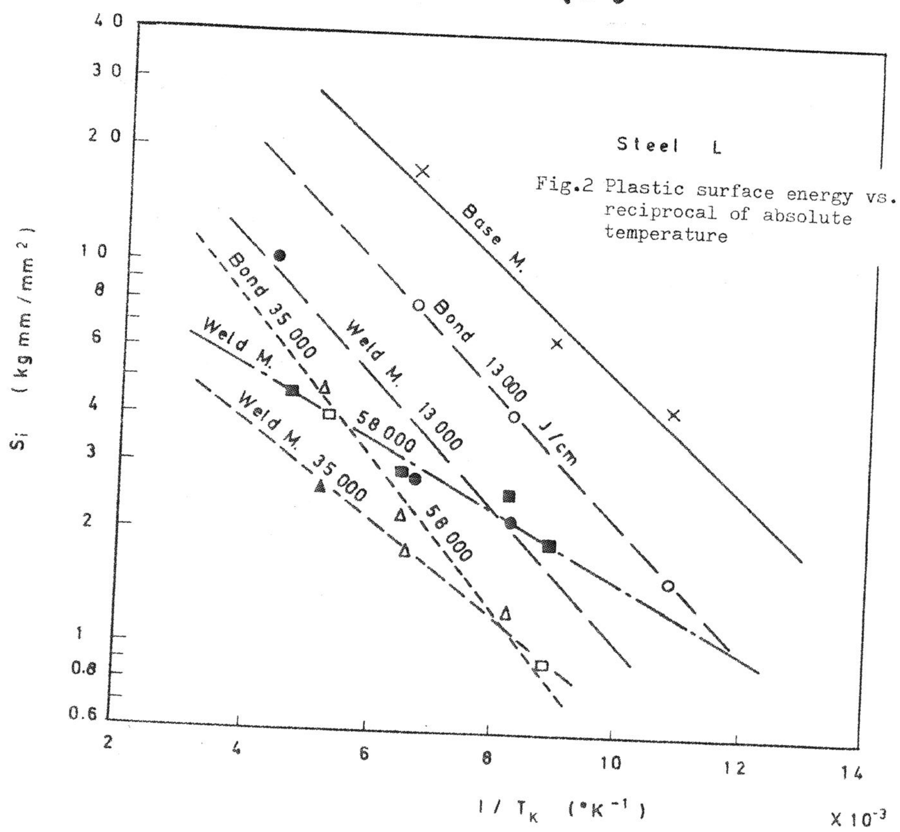

Fig.2 Plastic surface energy vs. reciprocal of absolute temperature

Steel	Kind of steel	Plate thickness (mm)	C
A	Normalized, killed	20	0.20
B	HW 36 (HT 60)	20	0.17
C	HW 40 (HT 60)	25	0.14
D	HW 63 (HT 70)	20	0.16
E	HW 50 (HT 70)	25	0.15
F	HW 70 (HT 80)	19	0.15
G	HW 80 (HT 80)	20	0.15
H	HW 90 (HT 100)	25	0.15
I	HW 90 (HT 100)	13	0.15
J	QT Al-killed 33	25	0.10
K	QT Al-killed 37	20	0.11
L	QT Al-killed 58	25	0.10
M	2.5% Ni	20	0.09
N	3.5% Ni	20	0.06
P	9% Ni	20	0.07
Q	Semi-killed	25	0.19
R	HW 50 (HT 60)	25	0.15
S	HW 63 (HT 80)	45	0.11
T	HW 70 (HT 80)	20	0.11

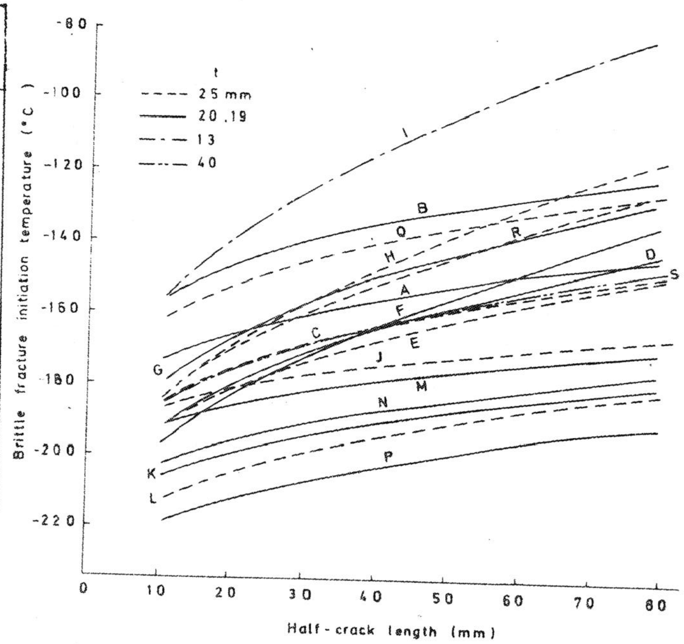

Fig.3 Brittle fracture initiation characteristics for various kinds of steel (base metal)

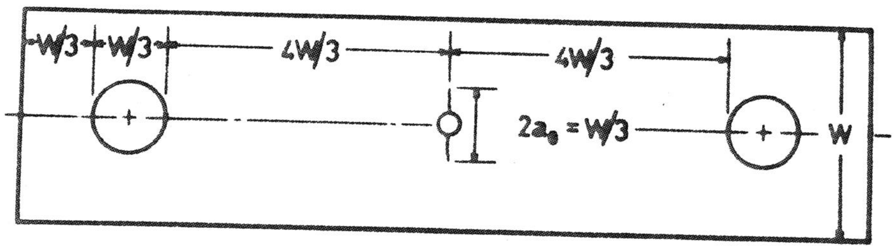

Fig.4 Center cracked specimen

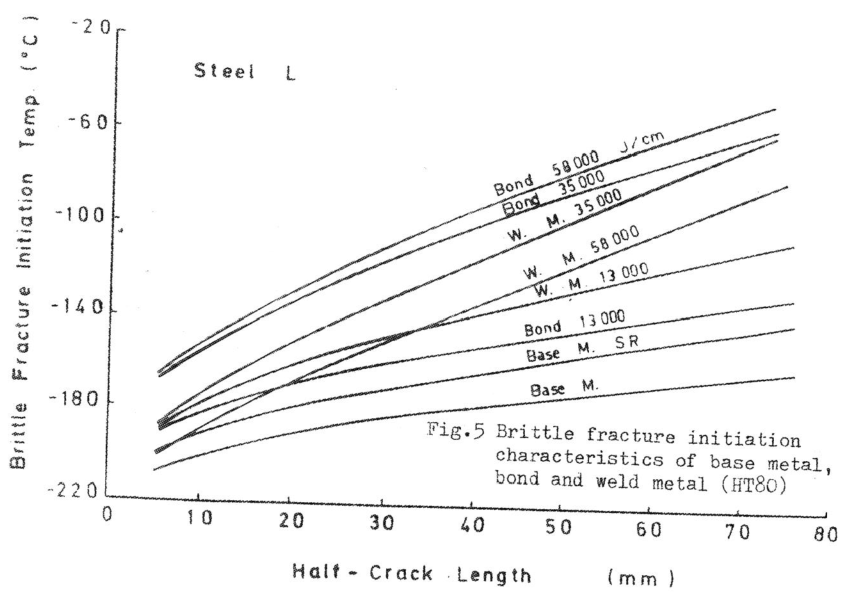

Fig.5 Brittle fracture initiation characteristics of base metal, bond and weld metal (HT80)

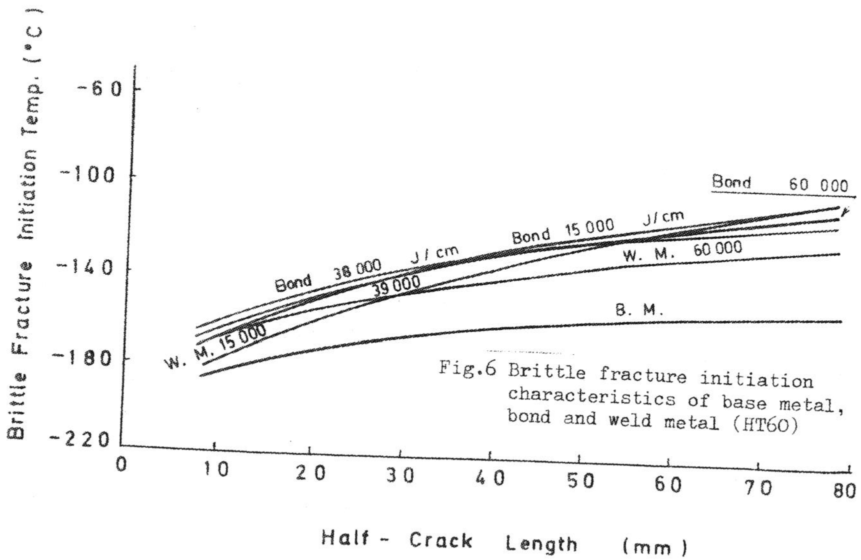

Fig.6 Brittle fracture initiation characteristics of base metal, bond and weld metal (HT60)

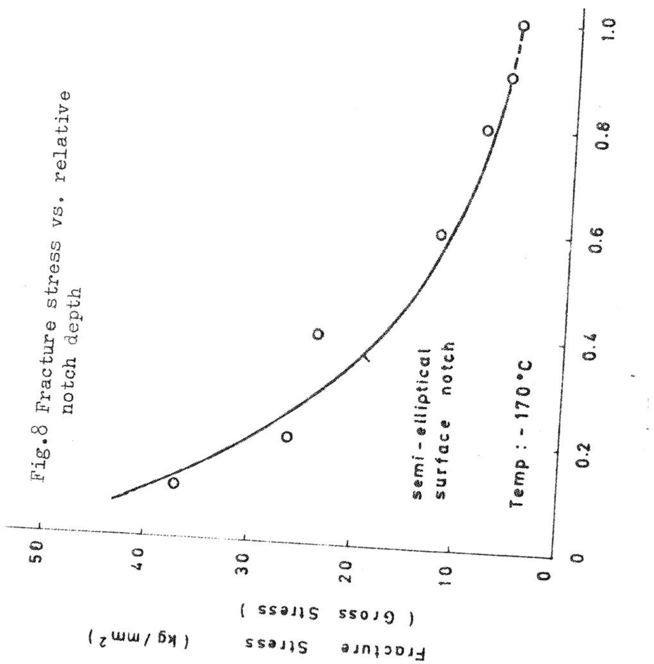

Fig.8 Fracture stress vs. relative notch depth

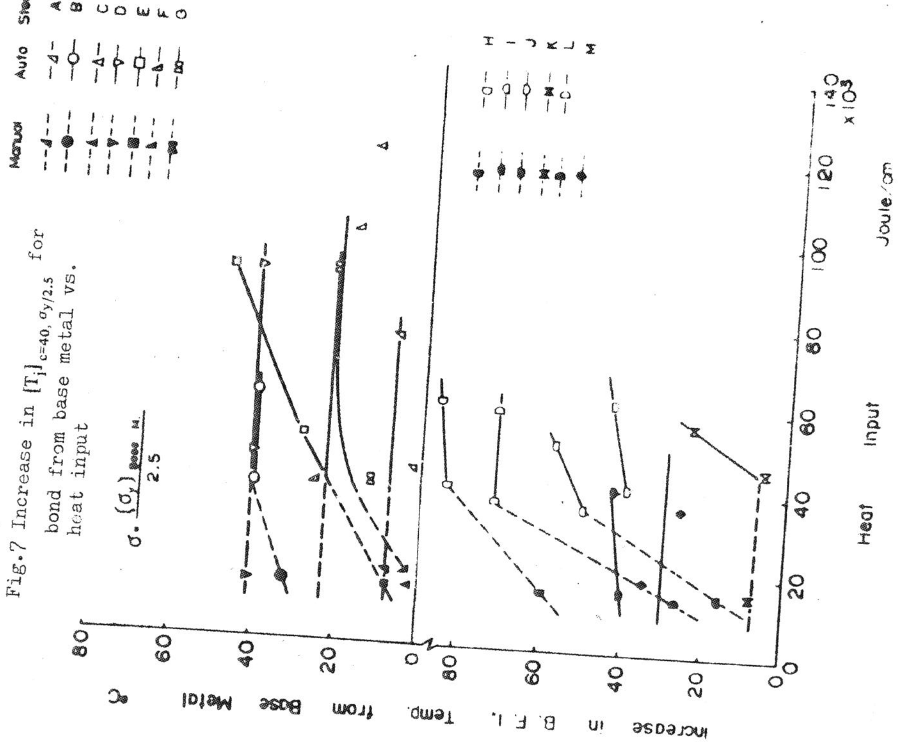

Fig.7 Increase in $[T_i]_{c=40,\ \sigma_y/2.5}$ for bond from base metal vs. heat input

$\sigma.\ \frac{(\sigma_y)_{Base\ M}}{2.5}$

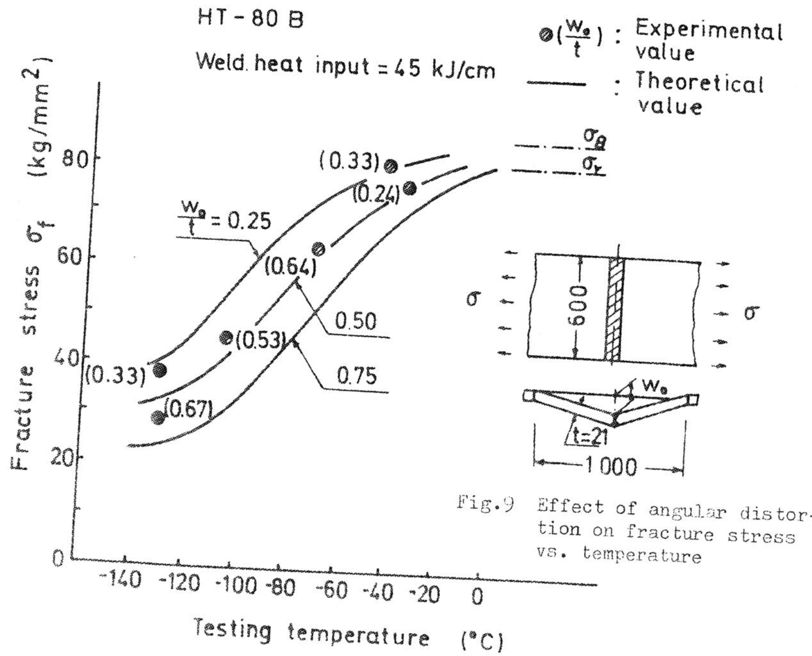

Fig.9 Effect of angular distortion on fracture stress vs. temperature

Fig.10 $f(\gamma)$, Y_B, κ_d and κ_e

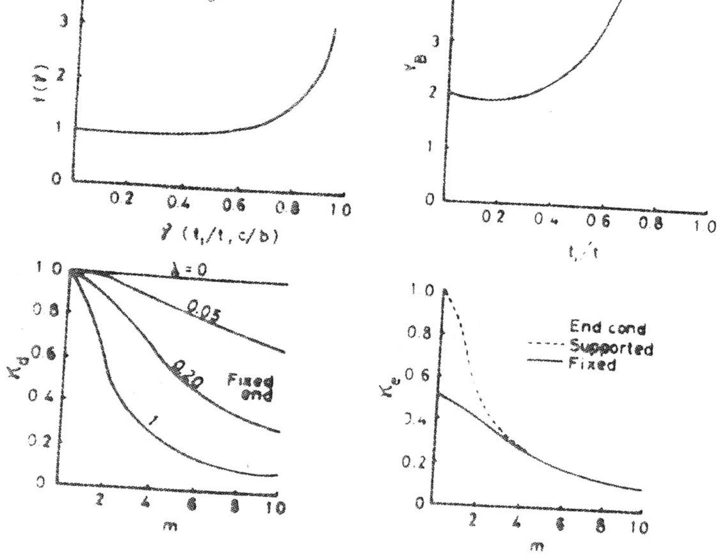

Steel	σ_y[a] (kg/mm²)	σ_1 (kg/mm²)	σ_1/σ_y	σ_2 (kg/mm²)	σ_2/σ_y
HT 60	50	42	0.84	53.7	1.08
HT 70	60	44	0.73		
HT 80	70	45	0.64	47.5	0.69
HT 100	90	48	0.53		

[a] Guaranteed yield point.

Table 1 Maximum residual tensile stress for longitudinal and cross joints, σ_1, σ_2.

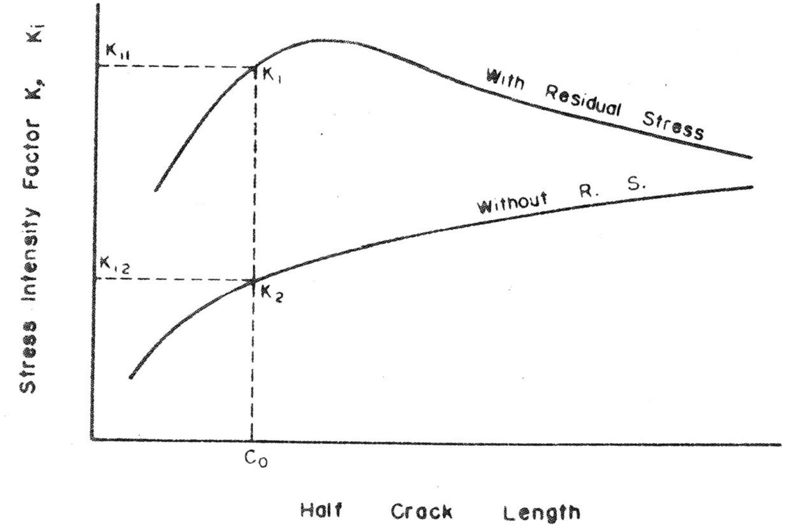

Fig.11 Effect of residual stress on K-C curve

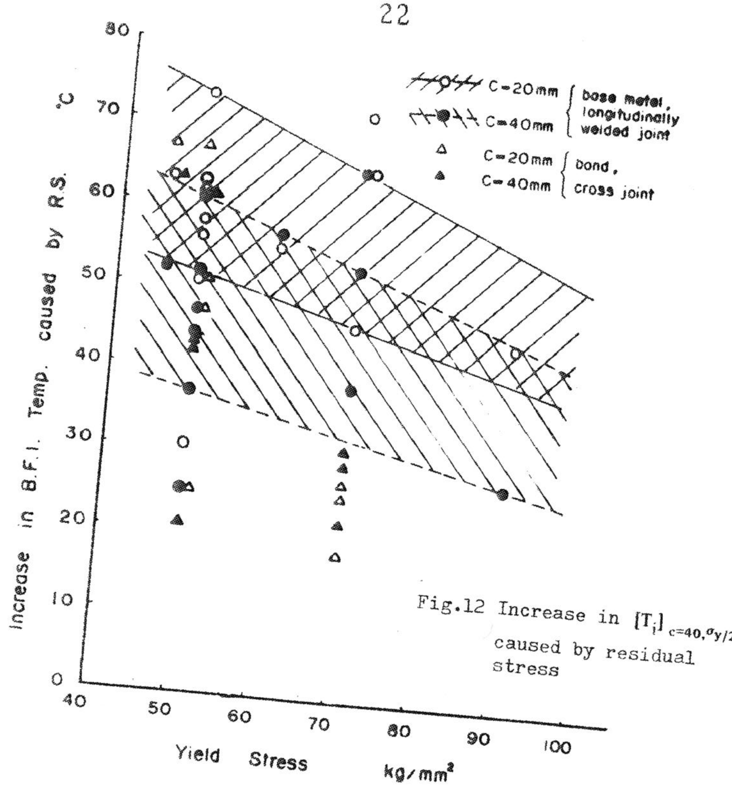

Fig.12 Increase in $[T_i]_{c=40,\sigma_y/2.5}$ caused by residual stress

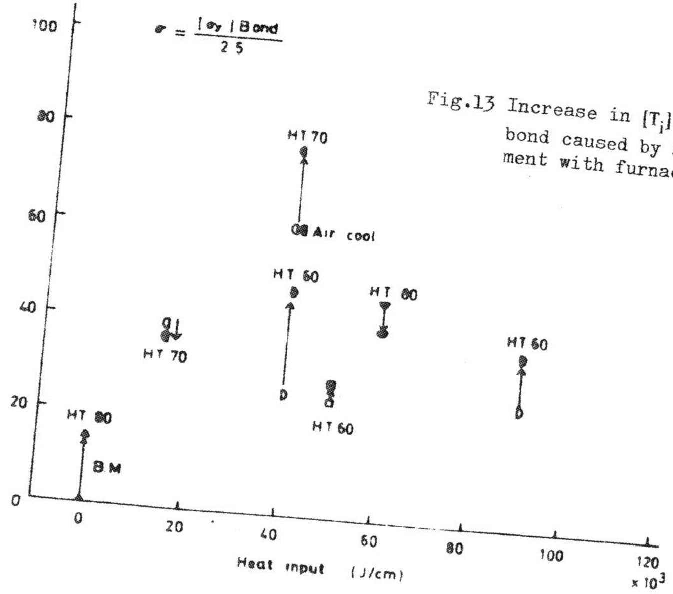

Fig.13 Increase in $[T_i]_{c=40,\sigma_y/2.5}$ of bond caused by S.R. treatment with furnace cooling

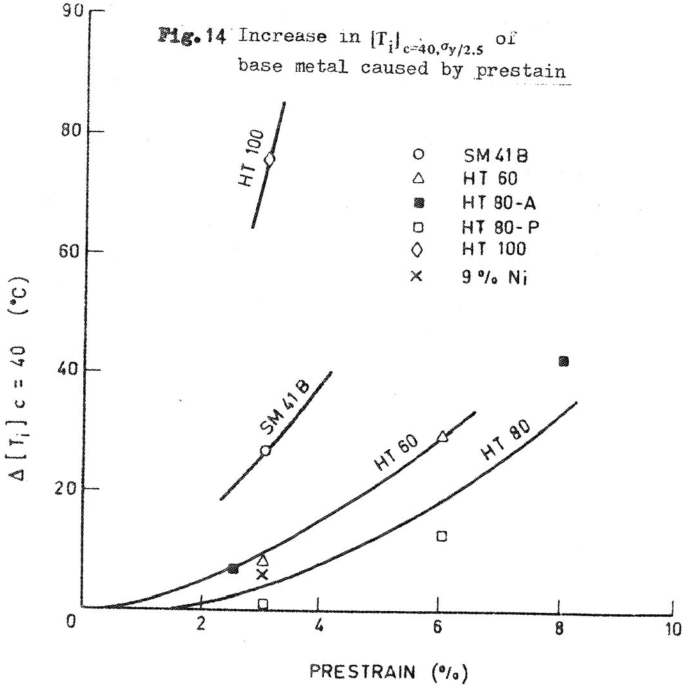

Fig.14 Increase in $[T_i]_{c=40,\sigma_y/2.5}$ of base metal caused by prestain

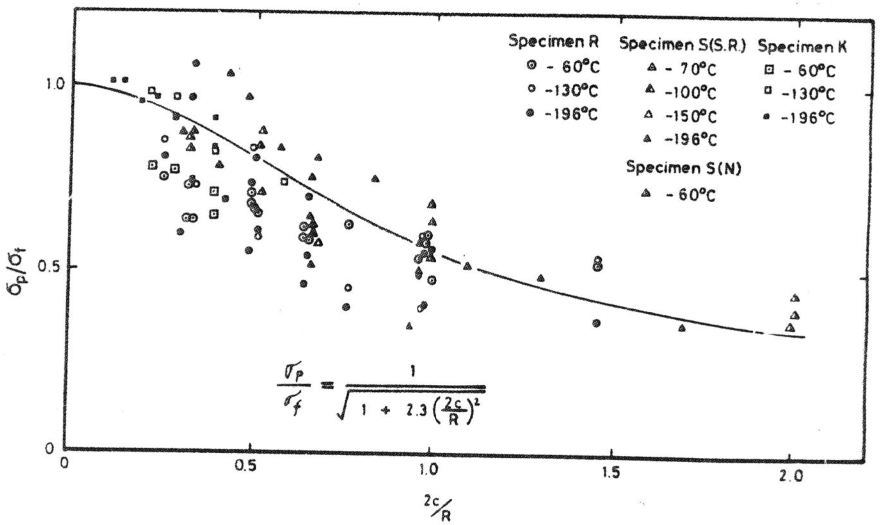

Fig. 15 $\sigma_{pipe}/\sigma_{flat}$ vs. $2c/R$

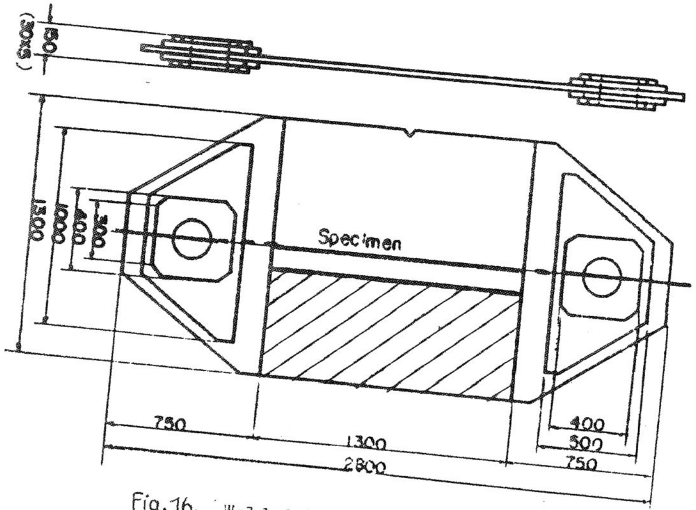

Fig. 16. Welded type crack arrester specimen

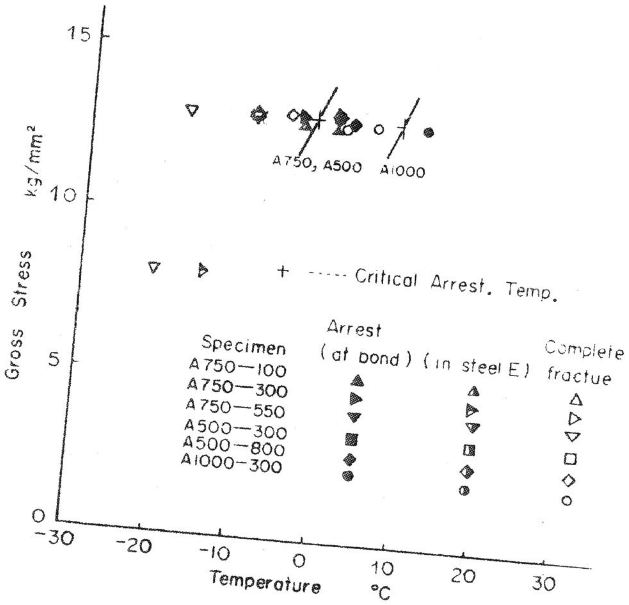

Fig. 17 Stress vs. propagation, arrest temperature for Grade E steel

PL VIII-411

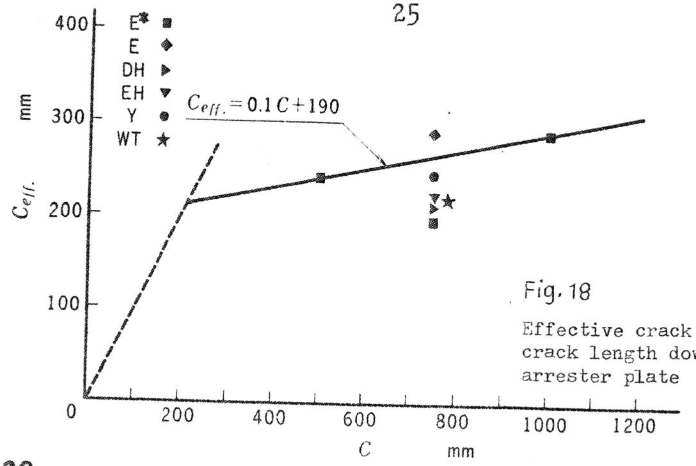

Fig. 18

Effective crack length vs. crack length down to arrester plate

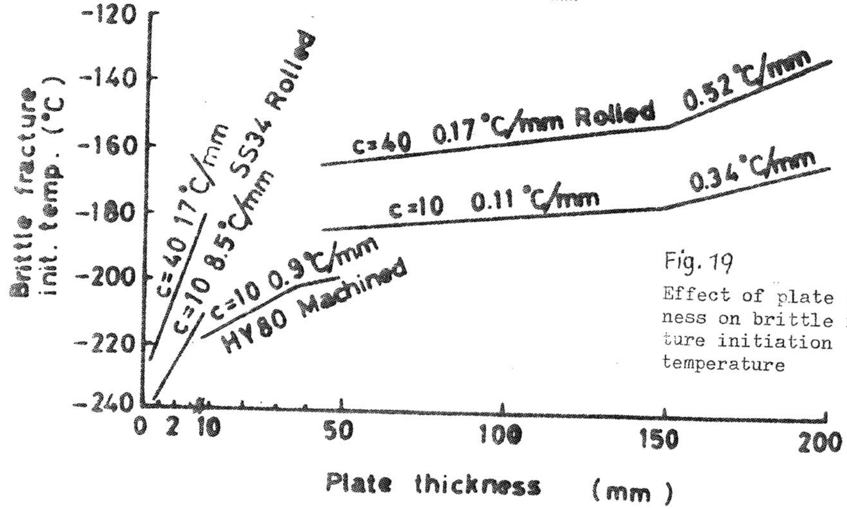

Fig. 19

Effect of plate thickness on brittle fracture initiation temperature

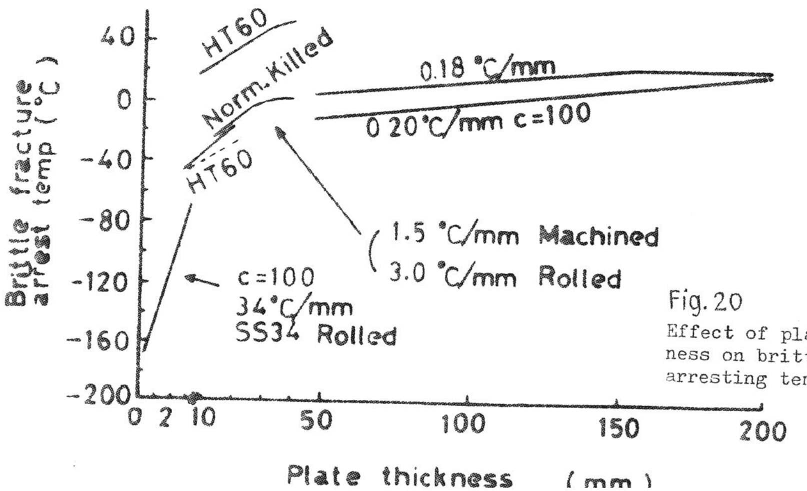

Fig. 20

Effect of plate thickness on brittle fractur arresting temperature